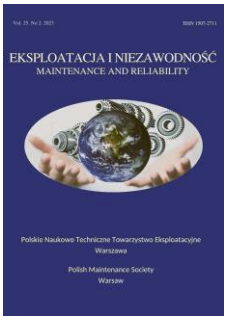

Eksploatacja i Niezawodnosc – Maintenance and Reliability

Volume 28 (2026), Issue 4

journal homepage: http://www.ein.org.pl

Article citation info:
Mei H, Liu X, Zhong Q, Duan R, Redundancy allocation optimization for k-out-of-n: G systems considering imperfect switching and uncertainty, Eksploatacja i Niezawodnosc – Maintenance and Reliability 2026: 28(4) http://doi.org/10.17531/ein/220119

Redundancy allocation optimization for *k*-out-of-*n*: G systems considering imperfect switching and uncertainty

Indexed by: Web of Science Group

Haipeng Mei[a], Xiwei Liu[b], Qi Zhong[a], Rongxing Duan[a,*]

[a] Nanchang University, China
[b] Macau University of science and technology, Macau

Highlights

- GSPN model for imperfect switching k-out-of-n systems under various redundancy strategies.
- Two-level sampling addresses both random uncertainty and epistemic uncertainty.
- A fixed-random-seed GA eliminates the impact of MCS errors on the optimization results.

Abstract

In safety-critical fields like energy and aerospace, optimizing system reliability is essential. This paper presents a novel Redundancy Allocation Problem (RAP) approach under component lifetime parameter uncertainties. By integrating Generalized Stochastic Petri Nets (GSPN) with Monte Carlo Simulation (MCS), a reliability evaluation framework is developed for k-out-of-n: G systems with imperfect switching, supporting active, cold standby, and mixed redundancy strategies. To jointly optimize component types, redundancy quantities, and strategies, a Genetic Algorithm with fixed-random-seed fitness evaluation eliminates Monte Carlo sampling variance, maximizing system reliability subject to cost and weight constraints. The proposed framework is validated through a case study on a natural gas compressor pipeline system. This work provides a quantitative decision-support tool enabling simultaneous selection of component types, redundancy levels, and strategies while characterizing solution reliability through confidence intervals under parameter uncertainty.

Keywords
redundancy allocation strategy, generalized stochastic petri nets, Monte Carlo simulation, fuzzy numbers, genetic algorithm

1. Introduction

Reliability is often the primary consideration in system optimization design, particularly when ensuring the safe operation of complex and costly equipment is essential [1,2]. Accordingly, reliability optimization design has become increasingly critical in modern high-tech sectors such as energy transmission, aerospace, and communications [3–5]. A central challenge in reliability engineering is the Redundancy Allocation Problem (RAP): determining the optimal number and configuration of redundant components for each subsystem, subject to cost and weight constraints, so as to maximize system-level reliability. Each component in a system is characterized by attributes such as type, reliability, cost, volume, and weight. Redundancy design involves selecting component types, redundancy strategies, and redundancy levels according to these attributes while considering system-level constraints such as reliability, cost, and other performance indicators. RAP represents a core challenge in reliability optimization. Since its introduction, it has attracted substantial research interest [6]. Solving the RAP necessitates not only determining the quantity of redundancy but also selecting the most appropriate type of redundancy strategy for each subsystem, as the choice of strategy profoundly influences system behavior and reliability.

(*) Corresponding author.
E-mail addresses: H. Mei (ORCID: 0009-0003-7362-6899) 416100240209@email.ncu.edu.cn, X. Liu (ORCID: 0009-0005-6793-4638) 1230003256@student.must.edu.mo, Q. Zhong (ORCID: 0009-0003-8742-3056) 416100230184@email.ncu.edu.cn, R. Duan (ORCID: 0000-0002-2886-1561) duanrongxing@ncu.edu.cn

Numerous studies have since extended and adapted the RAP formulation to accommodate diverse system architectures, component types, and practical constraints. Specifically, RAP seeks to identify the optimal redundancy numbers and strategies for each subsystem under constraints—especially cost and weight—so as to maximize overall system reliability [7]. To address engineering demands and enhance system reliability, researchers have extended the RAP model with respect to system architecture [8]. For 1-out-of-*n*: G systems within the RAP context, Guilani developed modeling and solution approaches based on Continuous-Time Markov Chains (CTMC) for mixed redundancy strategies [9]. Subsequent studies generalized these efforts to more complex *k*-out-of-*n*: G systems. Kim proposed a method for evaluating the reliability of *k*-out-of-*n*: G subsystems [10]; Jiang et al. introduced a reliability evaluation model using binary-addition [11]; and Zhang et al. put forward a CTMC-based reliability analysis technique [12]. Li and colleagues further developed CTMC-based modeling and computational methods for redundancy strategies across different system topologies [13].

Significant advancements have also been made in the development of redundancy strategies. Yeh et al. [14,15] developed system reliability models based on active redundancy strategies and applied corresponding methodologies to solve the resulting optimization problems. Oszczypała et al. [16,17], and Li et al. [18] constructed reliability models using cold standby redundancy strategies and employed intelligent optimization algorithms to address the redundancy optimization design problem. Zhang et al. [19], Reihaneh et al. [20], Gholinezhad et al. [21], and Peiravi et al. [22] incorporated redundancy strategies as decision variables, building system reliability models that incorporate active, mixed, and other redundancy strategies, and solved these models using appropriate optimization techniques. Peiravi et al. [7] further extended mixed strategies to K-mixed redundancy and provided corresponding model-solving methods. Ge et al. proposed a K-mixed redundancy strategy within a novel structural framework [23]. Long et al. proposed a Dynamic Mixed Heterogeneous Redundancy Strategy (DMHRS), which supports the dynamic adaptation of heterogeneous components and enables dynamic updates of redundancy configurations by optimizing the activation sequence of backup components and the switching time [24].

After defining the system structure and redundancy strategy, selecting a suitable reliability evaluation method is crucial. For systems with exponentially distributed component lifetimes, Zhang et al. [19], and Li et al. [25] developed reliability models based on Markov methods. Li et al. also proposed reliability models for systems with heterogeneous components under active, cold standby, mixed, and K-mixed redundancy strategies, employing CTMC for reliability assessment [26]. Additionally, Najmi et al. extended the RAP objective to a bi-objective optimization framework [27].

RAP has been established as an NP-hard problem [22]. Numerous studies have investigated various solution approaches and exact algorithms, including integer programming [28]. However, due to the computational limitations of exact methods—especially for large-scale problems—heuristic and metaheuristic algorithms have gained broader adoption. Commonly used metaheuristics include genetic algorithms [19], immune algorithms [29], particle swarm optimization [12,18], and cuckoo search algorithms [15], among others. Although substantial progress has been made in system structures, redundancy strategies, and optimization algorithms—including the design of diverse system topologies and subsystem configurations, the proposal of numerous redundancy strategies (from simple redundancy counts to various extended strategy formulations), and the development of methods ranging from approximate to exact and heuristic solutions—most existing studies assume that component attributes are deterministic. However, epistemic uncertainty plays a crucial role in engineering practice. It arises from incomplete knowledge, limited data, subjective expert judgment, and model simplifications, and is particularly prominent in early design stages or in safety-critical systems with insufficient data. Neglecting this uncertainty may lead to biased reliability estimates and overconfident decision-making.

Currently, only a few studies have attempted to incorporate epistemic uncertainty, using fuzzy or interval methods to characterize component parameters. Among these, Oszczypała et al. explored multi-objective reliability-redundancy allocation with active redundancy strategy [30]. Bakhtiari et al. extended the analysis to cold-standby redundancy [31]; however, their work still relies on the idealized assumption of perfectly reliable

fault detection and switching, failing to adequately account for the actual unreliability of switching mechanisms. This limitation restricts a realistic characterization of epistemic uncertainty in cold-standby and even mixed redundancy strategies.

To bridge these gaps, this paper proposes an integrated framework that combines GSPN, MCS, and a fixed-random-seed Genetic Algorithm (FS-GA) to solve the redundancy strategy selection problem for *k*-out-of-*n*: G systems under imperfect switching with consideration of epistemic uncertainty. The proposed framework is motivated by, and validated on, industrial energy infrastructure—specifically natural gas compressor pipelines—where reliable operation is mission-critical, component lifetime data are inherently limited, and redundancy decisions carry major safety and economic consequences. The main innovations and contributions of this paper are summarized as follows:

(1) To address the challenge of evaluating the reliability of *k*-out-of-*n*: G subsystems under various redundancy strategies in RAP, this paper proposes a novel reliability evaluation model based on GSPN, coupled with a solution approach using MCS.

(2) Given that the limited number of existing studies considering epistemic uncertainty are confined to a single redundancy strategy or rely on the idealized assumption of perfect fault detection and switching, this study incorporates uncertainty analysis into the redundancy strategy selection for *k*-out-of-*n*: G series-parallel systems with imperfect fault detection and switching, thereby forming a unified reliability evaluation framework for uncertain environments.

(3) To tackle the problem of redundancy strategy optimization under uncertainty, an FS-GA is developed to mitigate errors introduced by uncertainty during the GSPN-solving process with MCS, with the objective of identifying the optimal redundancy allocation strategy under uncertain conditions.

(4) To substantiate the engineering relevance of the proposed approach, the framework is applied to a real-world natural gas compressor pipeline system comprising six heterogeneous subsystems (pipeline, valves, filters, cooler, buffer tank, and liquid-gas separator). The results demonstrate that, compared with the deterministic benchmark approach, the proposed framework can identify the optimal system configuration under uncertainty in component lifetime parameters while providing confidence intervals for system reliability. This provides directly actionable support for reliability-maximizing design under simultaneous cost and weight constraints.

The remainder of this manuscript is structured as follows. Section 2 presents the reliability assessment framework, employing GSPN and MCS to characterize uncertainty in *k*-out-of-*n*: G subsystems under various redundancy configurations. Section 3 details the solution methodology for the optimization problem, utilizing a customized GA. Section 4 demonstrates the feasibility and accuracy of the proposed approach through a comprehensive engineering case study and comparative analysis. Finally, Section 5 concludes with key findings and directions for future research.

To ensure transparency and reproducibility, the key assumptions underlying the proposed framework are explicitly stated below:

Assumption 1 - Exponential lifetime distribution. Component lifetimes follow an exponential distribution characterized by a constant hazard rate lambda. This assumption is standard in system-level reliability studies for components.

Assumption 2 - Non-repairable system. The system is non-repairable within the mission time $T_{mission}$. This is representative of safety-critical systems such as aerospace or gas pipeline infrastructure where corrective maintenance cannot be performed during operation.

Assumption 3 - Independent component failures. Component failures are statistically independent.

Assumption 4 - Imperfect, time-dependent switching. The switching reliability is modelled as a time-dependent function $\rho(t_m)$ rather than a constant, capturing the progressive degradation of fault-detection mechanisms. Continuous monitoring is adopted throughout.

Assumption 5 - Triangular fuzzy numbers for epistemic uncertainty. The three vertices (θ_l, θ_m, θ_h) represent the lower bound, most likely value, and upper bound of the MTTF as assessed by domain experts or derived from sparse historical data. The triangular form is widely used in engineering fuzzy

reliability analysis.

2. Reliability evaluation model based on GSPN under uncertainty

2.1. Redundancy strategies of *k*-out-of-*n*: G Systems

This study investigates optimal redundancy strategies for non-repairable *k*-out-of-*n*: G systems under various constraints. In *k*-out-of-*n*: G systems, operational integrity is maintained provided that at least k components among n parallel units remain functional. Figure 1 illustrates a representative series-parallel configuration comprising m such subsystems.

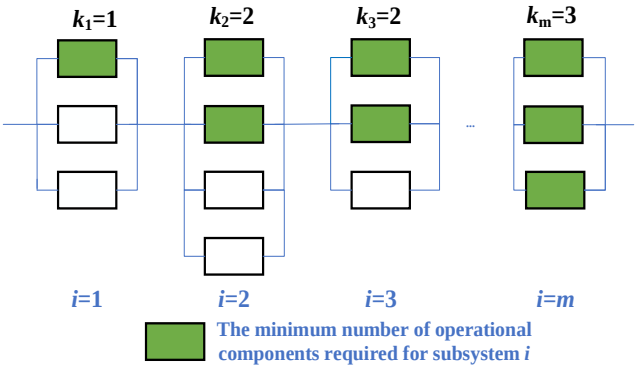

Figure 1. Series-parallel system composed of *k*-out-of-*n*: G subsystems.

For the *i*-th subsystem, n_{ai} denotes the number of active units, n_{si} represents the number of standby units, and k_i specifies the minimum threshold of operational components required for subsystem functionality. Table 1 presents four distinct redundancy strategies categorized by their respective combinations of (k_i, n_{ai}, n_{si}).

Table 1. Different redundancy strategies.

Scenarios	n_{ai}	n_{si}	Redundancy strategies
S1	$= k_i$	$= 0$	No Redundancy（N）
S2	$> k_i$	$= 0$	Active Redundancy (A)
S3	$= k_i$	> 0	Cold Standby Redundancy (S)
S4	$> k_i$	> 0	Mixed Redundancy (M)

To visualize the transition dynamics, Figure 2 demonstrates a 2-out-of-4: G system under mixed redundancy. Initially, the system operates with three active units and one standby unit. The degradation process involves five states: starting from full capacity (State 1), the system tolerates the first component failure (State 2). Upon a second failure (State 3), the detection mechanism triggers the standby unit to restore redundancy. However, subsequent failures eventually deplete the resources (State 4), leading to total system failure (State 5) when fewer than two components remain functional.

Implementing mixed redundancy necessitates a fault detection and switching system. Two primary operational logic types exist for switching system:

Case 1: Continuous monitoring is employed. Standby units are activated immediately when the number of active components falls below k_i. The switching reliability is modeled as a time-dependent function, $\rho_i(t_m)$.

Case 2: Switching occurs only at critical thresholds, with a constant success probability denoted by ρ_i.

The subsequent analysis focuses exclusively on Case 1.

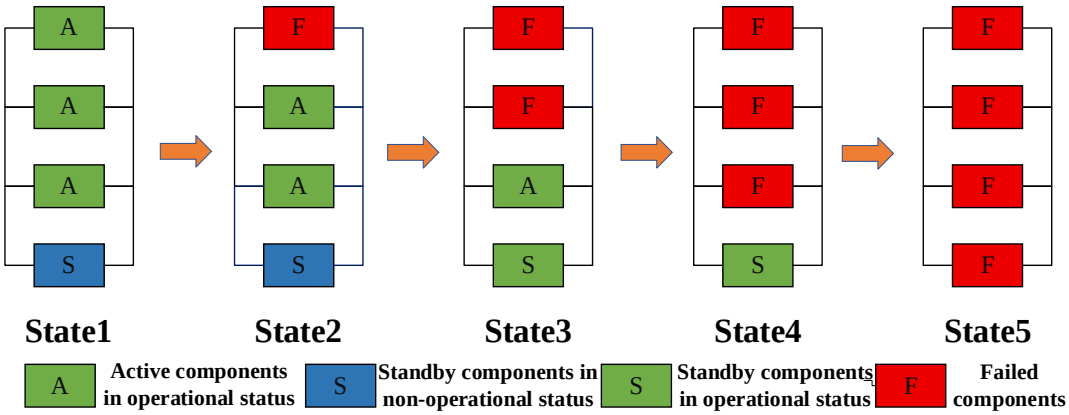

Figure 2. 2-out-of-4: G system with mixed redundancy strategy.

2.2. GSPN

Petri nets are a powerful graphical and mathematical modeling tool widely employed for representing and analyzing diverse systems [32]. A standard Petri net comprises four fundamental elements: places, tokens, transitions, and directed arcs. In reliability engineering, places—depicted as circles—represent the states of the system or its components. Tokens, typically represented as black dots, simulate the dynamic behavior of the system. Transitions, illustrated as rectangles, denote events that

cause the system to shift from one state to another. Directed arcs define the relationships between places and transitions, specifying the conditions and consequences of state changes. The weights labeled on the arcs indicate the number of parallel connections between nodes.

Traditional Petri nets are limited to modeling relatively simple system behaviors and lack the expressiveness required for complex systems. As a result, several extensions have been developed to enhance their descriptive and analytical capabilities. For instance, GSPN used in this study can effectively capture intricate dynamic behaviors and offers a comprehensive framework for modeling discrete-event dynamic systems. It has been extensively applied in reliability engineering [33]. The graphical notations of GSPN modeling elements are summarized in Table 2.

Table 2. Graphical elements of GSPN and their descriptions.

Graphical expressing	Description
	Place
	Immediate transition
	Timed transition
	Token
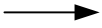	Directed arc
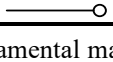	Inhibitor arc

The fundamental mathematical form of GSPN is defined in detail in reference [33].

To enhance the conciseness and flexibility of the GSPN model, this study employs a predicate/assertion-based extension of GSPN for system modeling. In this formalism, predicates—composed of one or more mathematical variables—are used to control the enabling conditions of transitions. When a transition fires, assertions modify the current variable assignments according to predefined rules, thereby updating the system state. In a GSPN, predicates are used to determine the truth value of conditions, and assertions are used to update variables, where,

Predicates (denoted by "??") are arbitrary formulas that can either be true or false. For example, "$??1 == 2$" is always false, and "$??x + 3 > 0$" is true when the result of the formula is positive, otherwise, it is false.

Assertions (denoted by "!!") are used to update the value of variables when transitions are triggered. For example, "$!!\, a = 3$" updates the value of a to 3, and "$!!\, M(p_2) = M(p_2) + 1$" increases the number of tokens in place p_2 by 1.

To enhance the clarity of the enabling and firing mechanisms in a predicate/assertion-extended GSPN model, an illustrative example is provided in Figure 3. In this model, place x_1 is linked to the immediate transition t_0 via an inhibitor arc. Place x_2 is connected to t_0 through an input arc of weight 1, and place x_3 via an input arc of weight 2. An output arc of weight 1 leads from t_0 to place x_5. The predicate of instantaneous transition t_0 is $??M(p_1) == 1$, and its assertion is $!!\, M(x_4) = M(x_4) + 1$. Additionally, place p_0 is connected to the timed transition t_1 by an input arc, while place p_1 is linked via an output arc. Place x_4 remains isolated in this configuration.

At initial time, the number of tokens in the three input places of transition t_0 is 0, 1, and 3, respectively, and the predicate evaluation results in false. The number of tokens in the input place of transition t_1 is 1. According to Definition 3, transition t_0 is not enabled at this point, while transition t_1 is enabled.

After a time interval t, timed transition t_1 fires, and the number of tokens in place p_1 becomes 1. This change in marking causes the predicate of t_0 to become true, enabling the immediate transition. Subsequently, t_0 fires without delay, increasing the token count in place x_5 to 1. Furthermore, the associated assertion updates the token count in place x_4 to 1.

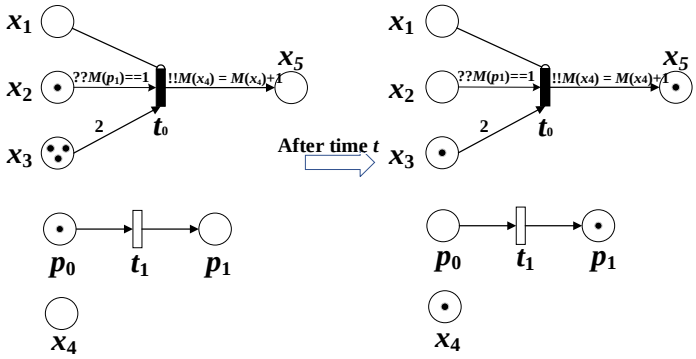

Figure 3. A simple example of GSPN.

2.3. Uncertainty

Aleatory uncertainty arises from inherent stochastic variations throughout the operational lifecycle of a product. These variations are primarily driven by environmental fluctuations, material degradation processes (e.g., fatigue), and random component failures [34,35]. In reliability engineering, component lifetime is modeled as a random variable characterized by specific probability distributions. Due to its analytical tractability and broad applicability, the exponential distribution serves as a foundational model for representing

component lifetimes.

The essential characteristics of this model—including the reliability function $R_{exp}(t)$, cumulative distribution function $F_{exp}(t)$, probability density function $f_{exp}(t)$, hazard rate $\lambda_{exp}(t)$, and mean time to failure ($MTTF_{exp}$)—are expressed mathematically in Eqs. (1)–(5):

$$R_{exp}(t) = exp(-\lambda t)(t > 0) \quad (1)$$

$$F_{exp}(t) = 1 - exp(-\lambda t)(t > 0) \quad (2)$$

$$f_{exp}(t) = \lambda exp(-\lambda t)(t > 0) \quad (3)$$

$$\lambda_{exp}(t) = \lambda \quad (4)$$

$$MTTF_{exp} = \frac{1}{\lambda_{exp}(t)} = \frac{1}{\lambda} \quad (5)$$

Epistemic uncertainty arises from subjective understanding, subjective judgment, and incomplete information. Due to the lack of data and insufficient understanding, the distribution parameters of the failure probability of components or systems are often not precise values. By introducing fuzzy numbers to express the epistemic uncertainty of the distribution parameters, reasoning and decision-making can be conducted based on incomplete information.

Let X be the space of fuzzy data points, and the general element of X is denoted by x, i.e.,$X = \{x\}$. A fuzzy set $\tilde{A}$ in X can be represented by a membership function$\mu\tilde{A}$:$X \rightarrow [0, 1]$, where the value of $\mu\tilde{A}(x)$ indicates the degree of membership of X in the fuzzy set $\tilde{A}$. A membership degree of $\mu(x) = 1$ or $\mu(x) = 0$ indicates that x fully belongs to or does not belong to $\tilde{A}$, respectively, while values between 0 and 1 represent partial membership.

Fuzzy numbers can take various forms; this study employs triangular fuzzy numbers. Let $x, a, b, c \in R$. A triangular fuzzy number $\tilde{A}$ can be represented as $\tilde{A} = (a, b, c)$, with its formula and graphical illustration shown in Table 3. When $x = a$ or $x = c$, the membership degree is $\mu(x) = 0$; when $x = b$, the membership degree is$\mu(x) = 1$. These two membership cases represent the boundary values and the most probable value of x, respectively.

Consider a complex system composed of n components. The failure probability of the system can be expressed as:

$$P(t) = Y(\theta; t) \quad (6)$$

where $\theta = [\theta_1, \theta_2, \theta_3, \ldots, \theta_n]$is the vector of parameters for the lifetime distributions of all components. For instance, θ_i represents the lifetime distribution parameter(s) for component i. To address the challenges posed by uncertainty, this paper represents the parameters of the component lifetime distribution as triangular fuzzy numbers $\theta = (\theta_l, \theta_m, \theta_h)$.

Table 3. Triangular fuzzy numbers.

	Expression	Legend
Triangular fuzzy numbers	$tri(x; a, b, c) = max\left\{min\left\{\frac{x-a}{b-a}, \frac{c-x}{c-b}\right\}, 0\right\}$	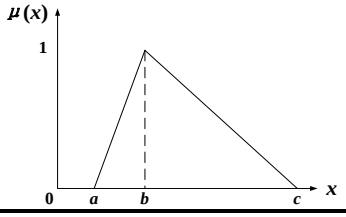

2.4. Modeling of *k*-out-of-*n*: G systems with different redundancy strategies under uncertainty using GSPN

Based on the failure modes and operational logic of *k*-out-of-*n*: G subsystems, the performance of the fault detection and switching mechanism is categorized into two distinct scenarios: Scenario 1: Successful switching operation. When the number of functional components falls below k_i, the workload is successfully transferred to a standby unit. Consequently, subsystem i remains operational until the standby reserve is exhausted, at which point the minimum requirement of k_i active units can no longer be maintained.

Scenario 2: Switching failure. When the number of operational components drops below k_i, the mechanism fails to activate standby units. This switching failure results in immediate subsystem i failure.

Taking a 2-out-of-4 system as an example, the applicable redundancy strategies include: Active redundancy (4 active components); Cold Standby redundancy (2 active components and 2 cold standby components); Mixed redundancy (3 active components and 1 cold standby component).

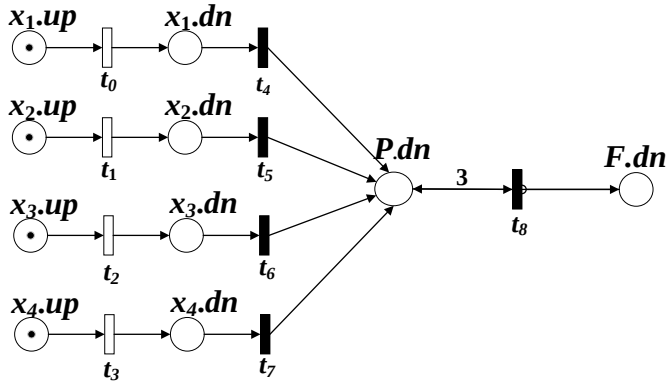

Figure 4. GSPN model of 2-out-of-4 system with active redundancy strategy.

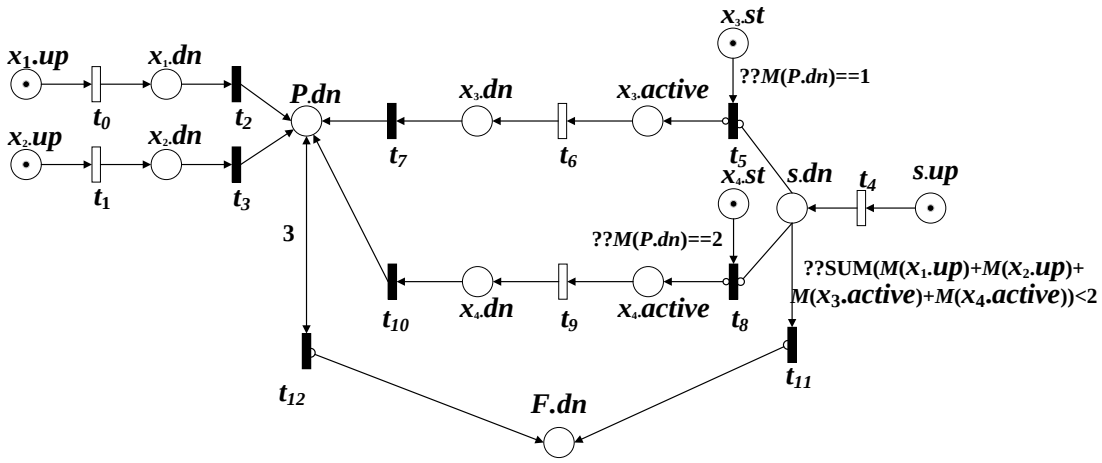

Figure 5. GSPN model of 2-out-of-4 system with cold standby redundancy strategy.

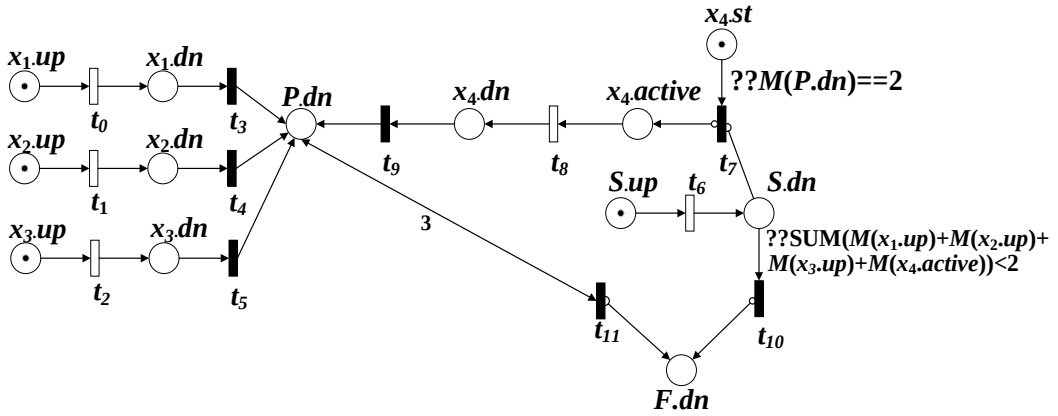

Figure 6. GSPN model of 2-out-of-4 system with mixed redundancy strategy.

Figures 4–6 present the GSPN models for a 2-out-of-4: G system under active, cold-standby, and mixed redundancy strategies, respectively. In all three models, the place *P.dn* accumulates tokens as components fail, and a token in *F.dn* signals system failure (i.e., fewer than $k = 2$ components remain operational). Under active redundancy (Figure 4), all four components operate simultaneously. System failure is triggered by immediate transition t_8 when *P.dn* reaches 3. Under cold-standby redundancy (Figure 5), two components are active and two are on standby. The predicates $??M(P.dn) == 1$ and $??M(P.dn) == 2$ sequentially activate the standby units (x_3, x_4) upon each failure, provided the switching system is functional(*S.up* holds a token). If the switching system fails (*S.dn* holds a token) and the number of operational components falls below 2 — i.e., the predicate $SUM\big(M(x_1.up) + M(x_2.up) + M(x_3.active) + M(x_4.active)\big) < 2$evaluates to

true — system failure is triggered immediately. Under mixed redundancy (Figure 6), three components are active and one is on standby. The first failure is tolerated without switching; the predicate $??M(P.dn) == 2$ triggers activation of x_4 upon the second failure. The same switching-failure logic as in Figure 5 applies: if $S.dn$ holds a token, the standby cannot be activated and the system fails immediately.

2.5. Evaluating the reliability of *k*-out-of-*n*: G systems under uncertainty

The two-layer sampling approach proposed in this section is intended to hierarchically represent both fuzzy and stochastic uncertainties. As depicted in Fig. 7, once a timed transition is enabled, its firing time is determined through two sequential sampling procedures, namely fuzzy parameter sampling and failure-time sampling. The corresponding timer then starts, and the transition fires only when the sampled firing time is reached. In the first sampling layer, the fuzzy parameter is characterized by a known membership function, whereas in the second layer, the failure time is described by a known cumulative distribution function. Accordingly, different sampling techniques are employed at the two layers.

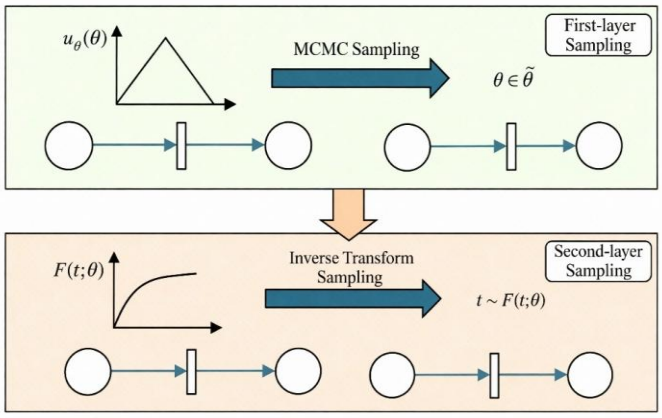

Figure 7. Schematic diagram of the two-layer sampling approach.

(1) MCMC sampling:

The Metropolis–Hastings algorithm is a Markov chain Monte Carlo (MCMC) technique designed to draw samples from probability distributions for which direct sampling is intractable. It constitutes a fundamental building block of many MCMC methods and is extensively employed to construct Monte Carlo samples that conform to a target distribution. Detailed descriptions and theoretical analyses of the algorithm are available in the literature [36,37].

The Metropolis-Hastings algorithm is as follows:

Algorithm: Metropolis–Hastings Sampling

Input: $P(x)$: Target distribution;
$Q(x' \mid x)$: proposal distribution, typically a Gaussian or another symmetric distribution;
N: Number of samples;
x_0: Initial sample, usually chosen as a representative point of $P(x)$.
Output: $\{x_k\}$: Sample sequence, k from 1 to N.

Begin:
//Initialization://
$k \leftarrow 0$ // initialize the sample index k as 0.
//Sampling://
Draw a candidate sample x' from the proposal distribution $Q(x' \mid x_k)$.
Draw a random number u from the uniform distribution $U(0, 1)$.
//Acceptance or Rejection//
Compute the acceptance probability:

$$\alpha(x', x_k) \leftarrow \min\left(1, \frac{P(x')Q(x_k \mid x')}{P(x_k)Q(x' \mid x_k)}\right).$$

If $u < \alpha(x', x_k)$ **Then**
accept x' as the next sample and set $\{x_{k+1}\} = x'$;
Else
reject x' and set $\{x_{k+1}\} = x_k$;
$k \leftarrow k + 1$
//Termination Condition//
If $k \geq N$ **Then**
output the sample sequence $\{x_k\}$;
Else
return to **Sampling**.
End

(2) Inverse transform sampling:

According to the probability integral transform theorem from probability theory: if a random variable X has a cumulative distribution function (CDF) of $F_X(X)$, then the random variable $U = F_X(X)$ follows a uniform distribution $U(0,1)$. The Inverse Transform Sampling method utilizes this property. By finding the inverse function of the CDF, $F_X^{-1}(U)$ (if it exists), a random sample $x = F_X^{-1}(u)$ from the target distribution can be obtained directly from a random number u generated from $U \sim U(0,1)$. Thus, the algorithmic steps for the inverse transform method can be written as:

(1) Generate a random number $u = U \sim U(0,1)$;

(2) Return the random number from the target distribution, $x = F_X^{-1}(u)$.

For stochastic uncertainty characterized by the exponential distribution, this study employs inverse transform sampling to convert uniformly distributed random numbers into samples following the target distribution, leveraging the fact that the exponential cumulative distribution function (CDF) is analytically invertible.

Under such uncertain conditions, the algorithm for evaluating system reliability in GSPN using MCS proceeds as follows:

Algorithm: Solving GSPN System Reliability using MCS

Input: *GSPN*: The mathematical form of the *GSPN=(P,T,I,O,H,W,M0)*;
T_mission: The mission time set for the system;
n: Total number of MCS.

Output: *R*: The reliability of the system within the mission time *T_mission*

Begin:
//Global Initialization://
n_f ← 0 // Initialize the failure counter *n_f* to 0. This variable counts the number of simulations that fail within the mission time.
//Monte Carlo Main Loop://
For *N* = 1 **to** *n* **do** //*N* is the index of the current simulation.
//Initialization for a Single Simulation Run//
M ← *GSPN.M0* //Reset the current system marking *M* to the model's initial marking *M0*.
T_current ← 0
W ← Sample_Delays(*GSPN.W*) // Perform random sampling for the delays of all timed transitions for the current simulation run.
//System State Evolution and Time Step//
While *T_current* < *T_mission* **and** *M(system_failure_place)* = 0 **do**
//Start the inner loop for a single simulation. The loop continues until the time exceeds the mission time or the system fails.
Enabled_Transitions ← Find_Enabled_Transitions(*M*) // Find all enabled transitions under the current system state *M*.
If *Enabled_Transitions* is empty **Then**//Check if there are any enabled transitions.
Break
End If
t_i ←Min_Time_Transition(*Enabled_Transitions, W*) // Select the one with the minimum firing time, *t_i*.
w_i ← Get_Firing_Time(*t_i*) // Get the firing time *w_i* of the selected transition, which will serve as the time step.
T_current ← *T_current* + *w_i* //Advance the current system time by the time step.
M ← Update_Marking(*M, t_i*) // Update the system marking *M* according to the firing rule of transition *t_i*.
End While
// Single Simulation Result Determination//
If *M(system_failure_place)* > 0 **and** *T_current* < *T_mission* **Then**
//Check if the system entered a failure state within the mission time at the end of this run.
n_f ← *n_f* + 1 //If the condition above is met, increment the failure counter *n_f* by 1.
End If
End For
//System Reliability Calculation and Return//
R ← 1 - (*n_f* / *n*) // Calculate the system's failure probability (*n_f* / *n*), then subtract it from 1 to get the reliability *R*.
Return *R*
End

In this section, we evaluate the reliability of the 2-out-of-4 systems under the redundancy strategies outlined in Section 2.4, incorporating both stochastic and epistemic uncertainties. The MTTF for both the components and the switching system is modeled as a triangular fuzzy number (515, 615, 715), and the mission time is set to 100 hours. The system reliability under uncertainty for each redundancy strategy is presented in Figures 8, 9, and 10, respectively.

In the figures, the blue curve represents the system reliability considering full uncertainty. The orange curve corresponds to the reliability at a membership level of α=1, where the MTTF is 615. The two gray curves indicate the reliability at the α=0 membership level, representing the lower and upper bounds of the fuzzy MTTF—515 and 715, respectively. As time progresses, the system reliability decreases gradually. The two $\alpha = 0$ curves define the envelope of possible reliability values under extreme parameter conditions, while the $\alpha = 1$ curve lies between them and reflects the scenario with the highest confidence. It is observed that the system reliability curve under full uncertainty (blue) closely aligns with the $\alpha = 1$ reference curve (orange). This experimental outcome confirms that the proposed method provides consistent and accurate reliability estimates under uncertainty, validating both the modeling approach and the solution technique introduced in this study.

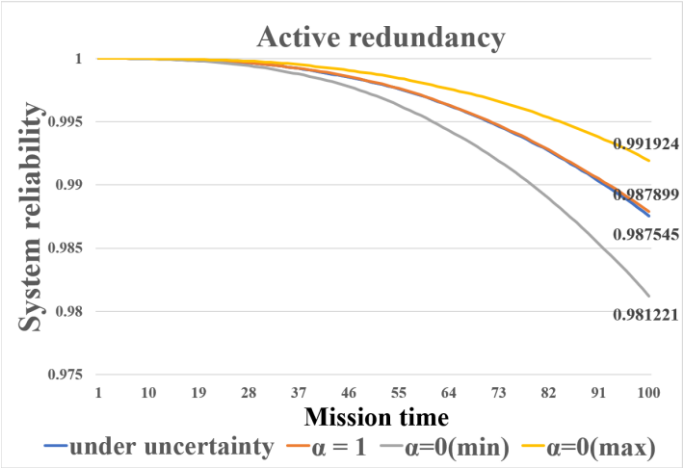

Figure 8. System reliability under active redundancy strategy considering uncertainty.

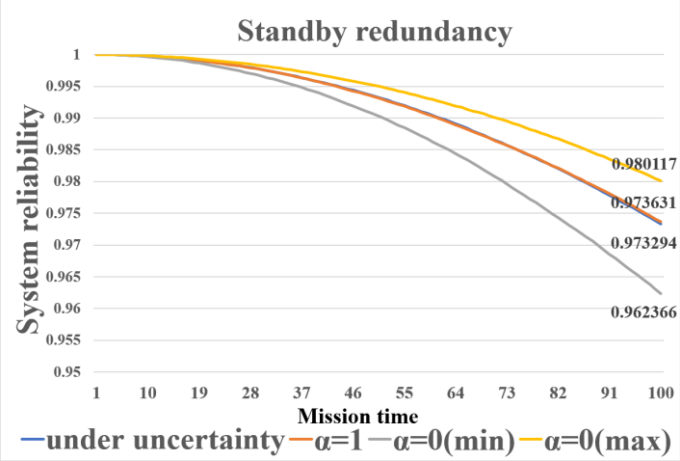

Figure 9. System reliability under cold standby redundancy strategy considering uncertainty.

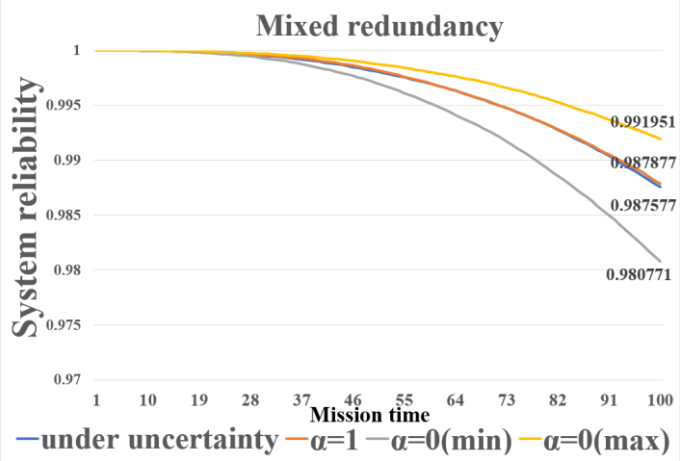

Figure 10. System reliability under mixed redundancy strategy considering uncertainty.

3. Solving RAP model

3.1. Description of RAP under uncertainty

The objective of this study is to determine the optimal system configuration by selecting appropriate component types, redundancy levels, and redundancy strategies to maximize overall system reliability under strict cost and weight constraints, while accounting for uncertainty in component lifetime parameters. The mathematical formulation of this optimization problem is presented in Eqs. (7)–(12):

$$max\ R_s = \prod_{i=1}^{m} R_i(t, k_i, n_{iz_i}^a, n_{iz_i}^s, \tilde{r}_{iz_i}) \quad (7)$$

$$s.t. \sum_{i=1}^{m} \sum_{z_i=1}^{u_i} (n_{iz_i}^a + n_{iz_i}^s) c_{iz_i} \le C_{max} \quad (8)$$

$$s.t. \sum_{i=1}^{m} \sum_{z_i=1}^{u_i} (n_{iz_i}^a + n_{iz_i}^s) w_{iz_i} \le W_{max} \quad (9)$$

$$\sum_{z_i=1}^{u_i} n_{iz_i}^a \ge k_i, \forall i = 1, \cdots, m \quad (10)$$

$$\tilde{r}_{iz_i} = (r_{iz_i}^l, r_{iz_i}^m, r_{iz_i}^h) \quad (11)$$

$$n_{iz_i}^a, n_{iz_i}^s \in N, \forall z_i = 1, \cdots, u_i, i = 1, \cdots, m \quad (12)$$

Where R_s represents the system reliability; R_i represents the reliability of the i-th k-out-of-n: G subsystem; t represents the mission time; k_i represents the minimum number of working components required for the i-th k-out-of-n: G subsystem; $n_{iz_i}^a$ represents the type of active components z_i in the i-th subsystem and the number of active components a in the i-th subsystem; $n_{iz_i}^s$ represents the type of standby components z_i in the i-th subsystem and the number of active components s in the i-th subsystem; c_{iz_i}represents the cost of a component of type in the i-th subsystem; w_{iz_i}represents the weight of a component of type in the i-th subsystem; C_{max} represents the maximum allowable cost for the system; W_{max} represents the maximum allowable weight for the system; $\tilde{r}_{iz_i}$represents the lifetime distribution parameter for components of type z_i in the i-th subsystem, which is expressed as the triangular fuzzy number$(r_{iz_i}^l, r_{iz_i}^m, r_{iz_i}^h)$.

3.2. Optimal solution of RAP under uncertainty using an FS-GA

GA is a search and optimization technique inspired by the principles of natural selection and genetics. As a heuristic method for locating optimal solutions, it is extensively used in reliability optimization [38]. This paper develops an FS-GA to address the problem of selecting the optimal redundancy strategy for k-out-of-n: G systems, as detailed below:

(1) Parameter configuration. The population size is set to *pop_size*, the number of generations to *evol_num*, the crossover rate to *crossover_rate*, and the mutation rate to *mutation_rate*. The chromosome length is 3**m*, where m is the number of subsystems, and the number of elites preserved is *elite_size*.

(2) Chromosome encoding. To represent solutions for the RAP, a structured chromosome is adopted, as illustrated in Figure 11. In this structure, z_i represents the component type for the i-th subsystem, n_{ai} represents the number of active components for the i-th subsystem, and n_{si} represents the number of standby components for the i-th subsystem.

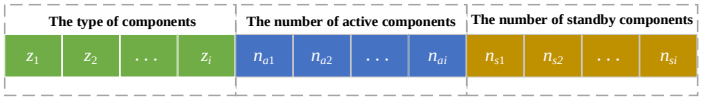

Figure 11. The structure of chromosome.

(3) Fitness calculation. For each chromosome, the values of z_i, n_{ai}, and n_{si} are used to construct a corresponding Petri net model from which subsystem reliability is computed. The

overall system reliability serves as the fitness value. Instead of a penalty function, explicit checks on weight and cost constraints for each subsystem are applied to ensure feasibility. It is important to note that when using MCS to evaluate the reliability of a GSPN model as part of the fitness function, stochastic uncertainty introduces evaluation variance. Even with identical chromosome encodings—within the same generation or across generations—repeated MCS evaluations may yield slightly different fitness values due to randomness. Typically, a very large number of simulations would be required to reduce this error. To mitigate this issue, this paper introduces a random seed control technique. Since computer-generated random numbers are pseudo-random—determined by an initial seed and a deterministic algorithm—using the same seed across all evaluations ensures that every individual is assessed using the same sequence of random numbers. This method effectively eliminates variability caused by the simulation process itself.

(4) Selection. Individuals are selected using the roulette wheel selection method, where the probability of selection for each individual is given by:

$$P_{\text{select}} = \frac{f_j}{\sum_{j=1}^{pop\_size} f_j} \tag{13}$$

where f_j denotes the fitness value of the j-th individual within the same population.

In particular, the purely random nature of the roulette wheel selection may cause the loss of superior individuals from the current generation, potentially leading to convergence at a local optimum or resulting in a situation where the best individual in the next generation is inferior to the best in the current one. To minimize this issue as much as possible, the number of individuals selected via the roulette wheel in each round is set to be smaller than *pop_size*. Then, the best individual from the current generation is placed into an experience pool to fill the remaining slots until the population size reaches *pop_size*. The newly filtered individuals are designated as new_pop.

(5) Crossover. A two-point crossover operator is applied with probability p_c exchanging segments between two parent chromosomes.

(6) Mutation. Each gene in the population is mutated with probability pm, introducing new genetic material to maintain diversity.

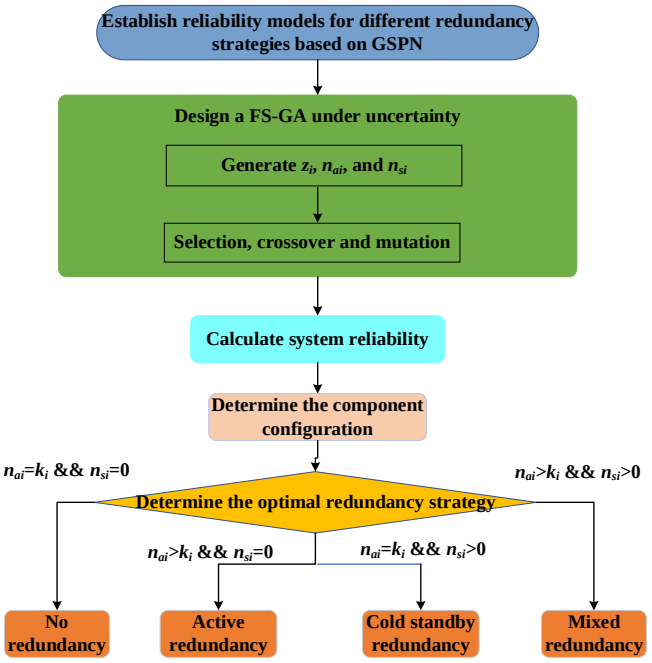

Figure 12. Flowchart for solving the optimal redundancy strategy.

The key enhancement over a standard GA lies not in modifying the selection, crossover, or mutation operators, but in controlling the random seed used by MCS during fitness evaluation. By fixing the seed, all individuals in the population—and across generations—are evaluated using an identical random number sequence, thereby eliminating Monte Carlo sampling variance as a source of noise in fitness comparison.

Figure 12 provides a flowchart of the proposed algorithm for determining the optimal redundancy strategy. The main steps are summarized as follows: First, subsystem reliability evaluation models are developed based on GSPN for different redundancy strategies—including active, cold standby, and mixed redundancy—while accounting for uncertainty. An FS-GA is then designed to compute system reliability under uncertain conditions. Next, an initial population is formed by randomly generating combinations of (z_i, n_{ai}, n_{si}), which represent system component configurations across various redundancy strategies. Subsequent generations are produced through selection, crossover, and mutation operations. In each generation, the system reliability of every individual is evaluated. Finally, after the algorithm converges, all solutions are compared to identify the maximum system reliability and the corresponding optimal redundancy strategy for each subsystem.

4. Case Study

4.1. RAP for the natural gas compressor pipeline system

To demonstrate the effectiveness and practical applicability of the proposed framework, a real-world engineering case involving a natural gas compressor pipeline system is examined. The schematic diagram of this series system is presented in Figure 13. Structurally, the system comprises a sequence of components: one pipe segment, three valves, two filters, one cooling unit, one buffer tank, and one liquid-gas separator. The natural gas compressor pipeline exemplifies safety-critical energy infrastructure with three characteristics that motivate the proposed framework: (a) the k-out-of-n: G architecture naturally models its subsystems (e.g., valves require at least 3 of n units); (b) component lifetime parameters are inherently uncertain due to sparse field data, typically estimated via expert elicitation; (c) unplanned downtime carries severe safety and economic consequences, making uncertainty-aware design essential. The framework simultaneously addresses component-type selection, redundancy level, and strategy choice for each of the six subsystems under fuzzy parameter uncertainty.

Consequently, reliability optimization under parameter uncertainty is critical. In this section, the GSPN-based reliability assessment and FS-GA optimization approach are applied to determine the optimal redundancy allocation strategy. The objective is to maximize system reliability while satisfying strict cost and weight constraints.

Each subsystem offers a choice of three component types, each characterized by distinct values of MTTF, weight, and cost. To achieve maximum system reliability under the given constraints, it is necessary to determine the optimal component type, quantity, and redundancy strategy for each subsystem. The lifetimes of both the components and the switching system are assumed to follow an exponential distribution. The reliability of the switching system is $\rho(t_m)$=0.99, and the mission time is 100 hours. The specific parameters for each component type in the subsystems are shown in Table 4, referenced from Zhang [19]. Using equations (1) to (5), the reliability values from the table are converted into the *MTTF* corresponding to a membership degree of α=1 in a triangular fuzzy number, which is also the middle value of that triangular fuzzy number.

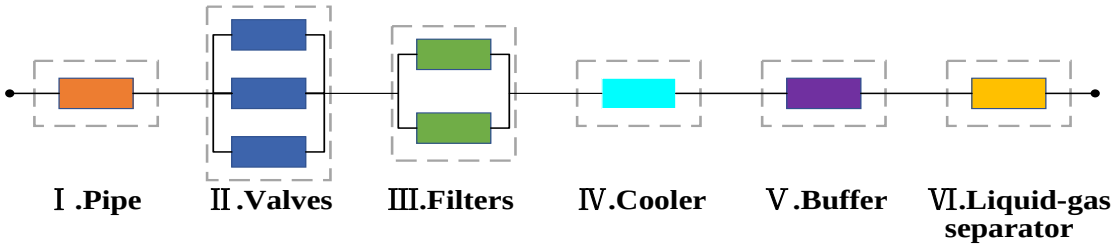

Figure 13. The natural gas compressor pipeline system.

Table 4. Parameters of the natural gas compressor pipeline system.

i	Subsystems	k_i	$MTTF_1$	c_{i1}	w_{i1}	$MTTF_2$	c_{i2}	w_{i2}	$MTTF_3$	c_{i3}	w_{i3}
1	Pipeline	1	(518,718,918)	6.85	10	(1000,1200,1400)	9.85	10	(1178,1378,1578)	10.85	12
2	Valves	3	(1750,1950,2150)	12.75	8	(4750,4950,5150)	14.35	9	(9750,9950,10150)	15.25	12
3	Filters	2	(1416,1616,1816)	10.85	8	(2250,2450,2650)	12.95	8	(4750,4950,5150)	15.15	10
4	Cooler	1	(415,615,815)	6.05	5	(750,950,1150)	8.05	5	(1178,1378,1578)	8.15	6
5	Buffer	1	(463,663,863)	9.35	4	(1000,1200,1400)	10.35	5	(1750,1950,2150)	10.85	7
6	separator	1	(415,615,815)	8.85	6	(1000,1200,1400)	10.25	6	(1416,1616,1816)	11.05	9

Table 5. Optimal solution for redundancy allocation when C_S = 160 and W_S = 130.

Constraints	parameters	Subsystem 1	2	3	4	5	6	W	C	Reliability	
C_S = 160 W_S = 130	z_i	1	1	1	1	3	3	159.2	123	$R(t_m)$	0.96919284
	n_{ai}	1	3	2	2	1	1			$R(t_m)_{\min}$	0.95310976
	n_{si}	1	1	1	1	1	1			$\bar{R}(t_m)$	0.96859370
	Strategy	S	S	S	M	S	S			$R(t_m)_{\max}$	0.97543891
	results from Zhang et al. [19]									$R^*(t_m)$	0.96700728

Table 6. Optimal solution for redundancy allocation when C_S = 180 and W_S = 150.

Constraints	parameters	Subsystem 1	2	3	4	5	6	W	C	Reliability	
C_S = 180 W_S = 150	z_i	1	2	1	3	3	2	179.85	136	$R(t_m)$	0.98936317
	n_{ai}	2	3	3	1	1	1			$R(t_m)_{\min}$	0.98490728
	n_{si}	1	1	1	1	1	1			$\bar{R}(t_m)$	0.98884068
	Strategy	M	S	M	S	S	S			$R(t_m)_{\max}$	0.99145842
	results from Zhang et al. [19]									$R^*(t_m)$	0.99506284

Table 7. Optimal solution for redundancy allocation when CS = 200 and WS = 180.

Constraints	parameters	Subsystem 1	2	3	4	5	6	W	C	Reliability	
C_S = 200 W_S = 180	z_i	1	3	1	1	3	3	197.95	166	$R(t_m)$	0.99679359
	n_{ai}	2	4	3	2	1	2			$R(t_m)_{\min}$	0.99218906
	n_{si}	1	0	1	1	1	1			$\bar{R}(t_m)$	0.99545811
	Strategy	M	A	M	M	S	M			$R(t_m)_{\max}$	0.99707330
	results from Zhang et al. [19]									$R^*(t_m)$	0.99506284

Table 8. Optimal solution for redundancy allocation when C_S = 220 and W_S = 180.

Constraints	parameters	Subsystem 1	2	3	4	5	6	W	C	Reliability	
C_S = 220 W_S = 180	z_i	1	3	1	3	3	2	219.55	177	$R(t_m)$	0.99848273
	n_{ai}	3	4	3	2	2	2			$R(t_m)_{\min}$	0.99773800
	n_{si}	1	0	1	1	1	1			$\bar{R}(t_m)$	0.99846486
	Strategy	M	A	M	M	M	M			$R(t_m)_{\max}$	0.99873056
	results from Zhang et al. [19]									$R^*(t_m)$	0.99839539

Table 9. Comparison Table of Methods.

	Zhang et al. [19]	This work
Component parameter uncertainty	Not considered	Incorporating triangular fuzzy numbers to address epistemic uncertainty.
Reliability modeling method	Based on CTMC, limited by state space explosion.	Based on GSPN, with excellent scalability.
Reliability output information	Point estimate reliability	Point estimate reliability + reliability bounds
Key advantages	Optimization of four redundancy strategies: *N*, *A*, *S*, *M*	Optimization of four redundancy strategies under uncertainty: *N*, *A*, *S*, *M*

The optimal redundancy allocation solutions for the natural gas pipeline system under uncertainty are summarized in Tables 5 to 8. Each table presents the best redundancy strategy and corresponding system reliability under a specific combination of cost and weight constraints. Here, C_S and W_S represent the upper limits for the total system cost and total system weight, respectively; z_i indicates the component type selected for the i-th subsystem, with three available types for each subsystem; n_{ai} represents the number of active components in the i-th subsystem; n_{si} represents the number of standby components in the i-th subsystem; The strategy column indicates the redundancy strategy adopted by each subsystem; $R(t_m)$ represents the best-estimated value of the system reliability for the optimal redundancy allocation solution under uncertainty; $R(t_m)_{\min}$ and $R(t_m)_{\max}$ represent the lower and upper bounds of the system reliability for the optimal redundancy allocation solution under uncertainty, respectively; $\bar{R}(t_m)$ represents the system reliability of the optimal redundancy allocation solution for the natural gas pipeline system under deterministic conditions, which is also the maximum possible value of the system reliability for the optimal solution under uncertainty. $R^*(t_m)$ represents the system reliability of the optimal redundancy allocation solution for the natural gas pipeline system under deterministic conditions as obtained by Zhang et al. [19].

The optimal redundancy strategy obtained in this study under deterministic conditions aligns with the results reported by Zhang et al. [19]. Moreover, the system reliability $\bar{R}(t_m)$ of

the optimal redundancy strategy selection under deterministic conditions is very close to the system reliability $R^*(t_m)$ of the optimal system redundancy allocation solution under deterministic conditions obtained by Zhang et al. [19]. This is sufficient to prove the accuracy and effectiveness of the method proposed in this paper for solving the RAP under deterministic conditions. Table 9 presents a multi-dimensional comparison between the method proposed in this paper and the method proposed by Zhang et al.

When uncertainty is incorporated, the best-estimated value of the system reliability, $R(t_m)$, lies between $R(t_m)_{\min}$ and $R(t_m)_{\max}$ and remains very close to $\bar{R}(t_m)$, which aligns with expectations. This is because the selected triangular fuzzy numbers are completely symmetrical. These results demonstrate that the proposed method can identify optimal redundancy strategies not only under deterministic conditions but also when uncertainty is considered.

From a reliability decision-making perspective, the results in Tables 5-8 provide actionable guidance at three levels:

(1) Component selection. The framework consistently selects lower-cost component types for subsystems with lower ki thresholds, reserving premium components for bottleneck subsystems where redundancy alone is insufficient. This enables efficient allocation of procurement budgets.

(2) Strategy selection under budget pressure. Under tight constraints ($C_S = 160$, $W_S = 130$), S strategy dominates for most subsystems because it maximizes redundancy depth within the permitted component count. As constraints relax, M strategy and A strategies appear where higher intrinsic reliability justifies additional active components.

(3) Uncertainty-aware risk assessment. The reliability confidence interval [$R(t_m)_{\min}$, $R(t_m)_{\max}$] provides explicit best-case and worst-case performance bounds. For safety-critical certification, the lower bound $R(t_m)_{\min}$ should be used as the conservative design criterion. The interval width directly reflects the degree of epistemic uncertainty: a wide interval signals that more precise lifetime data are needed before finalizing the design.

As shown in Figures 14 and 15, relaxing the constraints on total cost and total weight results in an increase in the total number of system components. This, in turn, leads to higher redundancy levels and a subsequent improvement in system reliability.

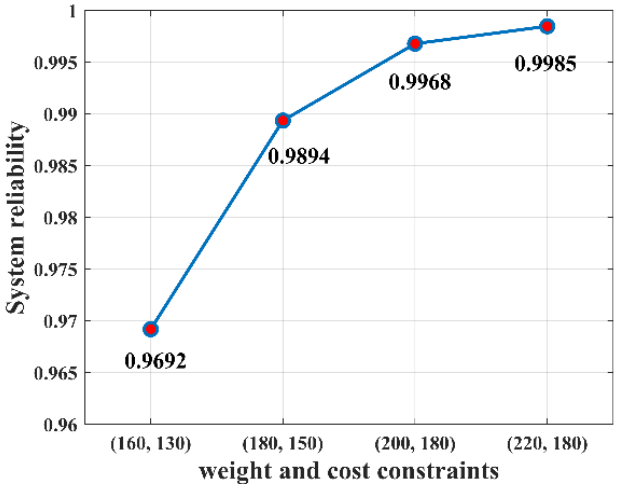

Figure 14. System reliability under different constraints.

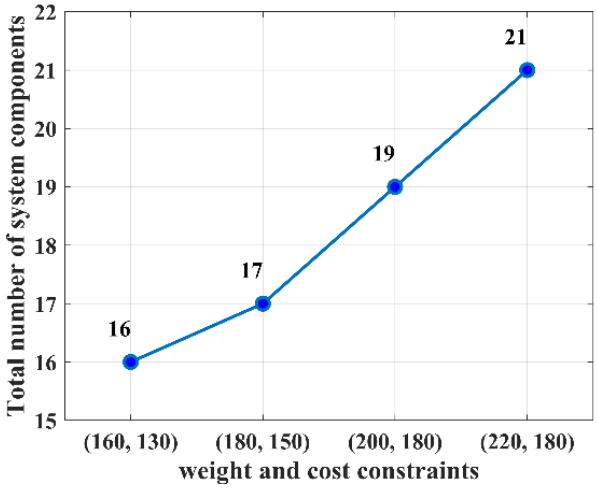

Figure 15. Total number of system components under different constraints.

Beyond the natural gas compressor pipeline, the proposed framework is directly applicable to other safety-critical *k*-out-of-*n*: G systems in which component lifetime data are sparse, such as aerospace actuator assemblies, nuclear instrumentation systems, and offshore wind turbine subsystems — any domain where conservative, uncertainty-aware redundancy design is operationally essential.

4.2. Comparative analysis with traditional GA under uncertainty

To further demonstrate the superiority of the proposed FS-GA over a standard GA, comparative experiments were conducted under the same uncertain environment. Figure 16 compares the performance of a traditional GA and the FS-GA proposed in this study (under the conditions of C_S = 160 and W_S = 130). As shown in Fig. 16, the standard GA exhibits persistent fitness fluctuations across all 200 generations due to Monte Carlo

sampling variance in the fitness evaluation, making it impossible to reliably identify the best individual in any given generation. In contrast, the FS-GA incorporates a fixed random seed to eliminate stochastic simulation variance, thereby achieving stable and repeatable fitness evaluations, which is critical for trustworthy decision-making.

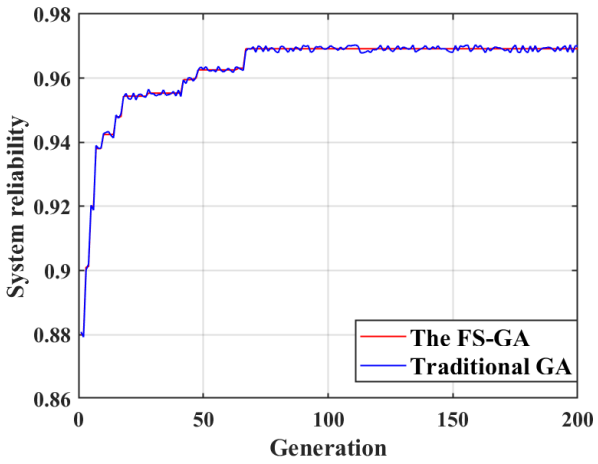

Figure 16. System reliability results calculated using the FS-GA and traditional GA.

4.3. Robustness analysis: symmetric vs. asymmetric fuzzy numbers

A key advantage of the proposed method is its ability to handle various forms of epistemic uncertainty. To test its robustness, we conducted experiments using the asymmetric triangular fuzzy numbers for MTTF and compared the results with those derived under symmetric fuzzy assumptions, keeping all other constraints identical (C_S = 160 and W_S = 130). When asymmetric fuzzy numbers are used, the defuzzification via the centroid method may yield an equivalent mean failure time that deviates from the most plausible value (the center of the fuzzy set). As a result, the estimated system reliability may differ more significantly from the maximum achievable value. To illustrate this effect, we reconfigured the system parameters using the asymmetric fuzzy numbers detailed in Table 10, while holding all other conditions constant.

As shown in Table 11, the optimal redundancy strategy under asymmetric uncertainty differs from that obtained under symmetric assumptions. A further observation from Table 11 is that the best-estimated system reliability $R(t_m)$ under asymmetric uncertainty (0.97103) exceeds that under symmetric assumptions (0.96919). The mechanism is as follows.

Table 10. System parameters with asymmetrical triangular fuzzy numbers.

i	Subsystems	k_i	$MTTF_1$	c_{i1}	w_{i1}	$MTTF_2$	c_{i2}	w_{i2}	$MTTF_3$	c_{i3}	w_{i3}
1	Pipeline	1	(618,718,918)	6.85	10	(1100,1200,1400)	9.85	10	(1278,1378,1578)	10.85	12
2	Valves	3	(1850,1950,2150)	12.75	8	(4850,4950,5150)	14.35	9	(9850,9950,10150)	15.25	12
3	Filters	2	(1516,1616,1816)	10.85	8	(2350,2450,2650)	12.95	8	(4850,4950,5150)	15.15	10
4	Cooler	1	(515,615,815)	6.05	5	(850,950,1150)	8.05	5	(1278,1378,1578)	8.15	6
5	Buffer	1	(563,663,863)	9.35	4	(1100,1200,1400)	10.35	5	(1850,1950,2150)	10.85	7
6	separator	1	(515,615,815)	8.85	6	(1100,1200,1400)	10.25	6	(1516,1616,1816)	11.05	9

Table 11. System optimal solution under asymmetric fuzzy numbers.

Constraints	parameters	Subsystem 1	2	3	4	5	6	W	C	Reliability	
					the result of this paper						
C_S = 160 W_S = 130	z_i	1	1	1	1	3	3	159.2	123	$R(t_m)$	0.97102878
	n_{ai}	1	3	2	3	1	1			$R(t_m)_{\min}$	0.96409378
	n_{si}	1	1	1	0	1	1			$\bar{R}(t_m)$	0.96907162
	Strategy	S	S	S	A	S	S			$R(t_m)_{\max}$	0.97634959
					results from Zhang et al. [19]						
C_S = 160 W_S = 130	z_i	1	1	1	1	3	3	159.2	123	$R^*(t_m)$	0.96700728
	n_{ai}	1	3	2	2	1	1				
	n_{si}	1	1	1	1	1	1				
	Strategy	S	S	S	M	S	S				

For a triangular fuzzy number (a, b, c), the centroid is (a + b + c) / 3. In Table 10, the lower bound a of every component type is raised by exactly 100 hours relative to Table 4, while b and c are unchanged. This uniformly shifts each centroid upward by 100/3 = 33.3 hours. Therefore, the average failure rate of each component, λ = 1/MTTF, will decrease, resulting in

higher average reliability.

Because the MCMC sampling in the first layer draws failure-rate values theta according to the membership function, the average sampled lambda under asymmetric TFNs is systematically lower than under symmetric TFNs. Through $R(t) = \exp(-\lambda \cdot t)$, this lower average failure rate propagates to a higher system-level best-estimate reliability.

In physical terms, the asymmetric TFNs encode an expert belief that component lifetimes are unlikely to be as short as the worst case assumed in the symmetric parameterization (i.e., the lower bound is raised from 415 to 515 h for subsystem 4 type 1). This less pessimistic characterization of uncertainty naturally produces a higher best-estimate system reliability. It also changes the cost-benefit balance between redundancy strategies, as explained above. Designers should therefore carefully assess the shape—not only the central value—of their uncertainty characterizations before selecting a redundancy strategy.

5. Conclusion

This paper proposes an integrated GSPN–MCS–FS-GA framework for the Redundancy Allocation Problem of k-out-of-n: G series-parallel systems under epistemic uncertainty in component lifetime parameters. The GSPN model captures the state-transition dynamics of subsystems across active, cold-standby, and mixed redundancy strategies; MCS evaluates system reliability under dual (aleatory + epistemic) uncertainty; and the fixed-seed genetic algorithm eliminates Monte Carlo sampling variance from fitness evaluation, enabling reliable optimization. Compared with deterministic approaches such as [19,22], the framework simultaneously identifies optimal component types, redundancy quantities, and strategies while providing reliability confidence intervals.

The core contribution of this work lies in the first-of-its-kind integration of GSPN, MCS, and the FS-GA into a unified framework for RAP under uncertainty. This integration provides the following advantages:

(1) A more flexible and accurate reliability evaluation of complex systems under various redundancy strategies (active, cold standby, mixed), surpassing the limitations of traditional analytical methods.

(2) The simultaneous optimization of component type, redundancy level, and strategy under cost and weight constraints, even when distribution parameters are imprecise.

(3) Demonstrated superior stability and convergence in optimization compared to traditional GAs, which often fluctuate under uncertainty.

The practical value of the proposed approach is validated through a real-world case study on a natural gas compressor pipeline system. The results are generally consistent with the deterministic benchmark solution reported in [19], and in some constraint settings the proposed framework yields competitive or slightly improved reliability performance while additionally providing uncertainty-aware reliability bounds. Concretely, the framework delivers three levels of engineering decision support for pipeline system designers: (i) component procurement guidance, by identifying which component type offers the best reliability-per-unit-cost ratio for each subsystem; (ii) redundancy strategy selection under budget constraints, showing that cold-standby strategies dominate under tight cost limits while mixed strategies emerge as constraints relax; and (iii) uncertainty-aware risk quantification, where the reliability confidence interval $[R(t_m)_{\min}, R(t_m)_{\max}]$ reported in Tables 5–8 provides an actionable conservative bound for safety certification purposes. The interval width also serves as a direct diagnostic: a wide interval signals that more precise lifetime data are needed before the design can be safely finalized. These outputs are not available from classical deterministic RAP solvers and represent a tangible advancement for safety-critical infrastructure planning.

Future research will focus on addressing the following important issues: (1) The Reliability-Redundancy Allocation Problem (R-RAP) for complex systems with k-out-of-n:

G subsystems and heterogeneous components: Future studies will extend the current model to accommodate systems composed of components with varying performance characteristics and lifetime distributions, improving the model's precision and applicability. (2) Integration of component degradation and redundancy optimization: Given that components may degrade over time in real applications, future research will incorporate degradation models into redundancy allocation to maintain long-term system reliability. (3) Joint optimization of maintenance and redundancy resources: System reliability relies not only on redundancy allocation but also on maintenance strategies. Future work will explore the integrated

optimization of maintenance and redundancy resources to minimize lifecycle costs while ensuring high reliability under uncertainty. (4) Comprehensive parametric sensitivity analysis. The robustness analysis in Section 4.3 provides initial evidence of the framework's sensitivity to the shape of the input uncertainty characterization. Future work will extend this to a systematic parametric study examining the influence of switching reliability ρ(tm), the spread and skewness of the fuzzy MTTF distributions, and constraint tightness on the optimal redundancy configuration and reliability bounds, with the aim of providing practitioners with quantitative guidance on which parameters most critically affect design decisions.

References

1. Friederich J, Lazarova-Molnar S. Reliability assessment of manufacturing systems: A comprehensive overview, challenges and opportunities. Journal of Manufacturing Systems 2024; 72: 38–58. https://doi.org/10.1016/j.jmsy.2023.11.001.
2. Singla S, Mangla D, Kumar M A, Muhammad M U. Reliability optimization methods: A systematic literature review. Yugoslav Journal of Operations Research 2025; 35(1) :1–30. https://doi.org/10.2298/YJOR230715031S.
3. Kumar B V, A A F M. Optimal Simultaneous Allocation of Electric Vehicle Charging Stations and Capacitors in Radial Distribution Network Considering Reliability. Journal of Modern Power Systems and Clean Energy 2024; 12(5): 1584–95. https://doi.org/ 10.35833/MPCE.2023.000674.
4. Wang J, Yin Y, Qu J, Chen H, Lian X. Situation modeling and evaluation for complex systems: A case study of satellite attitude control system. Advanced Engineering Informatics 2024; 61: 102505. https://doi.org/10.1016/j.aei.2024.102505.
5. Chen Z, Zhang H, Wang X, Yang J, Dui H. Reliability analysis and redundancy design of satellite communication system based on a novel Bayesian environmental importance. Reliability Engineering & System Safety 2024; 243: 109813. https://doi.org/10.1016/j.ress.2023.109813.
6. Guan B, Li Z, Coit D W, Li Y F. Review of the redundancy allocation problem to optimize system reliability. Engineering Optimization 2025; 57(1): 44–68. https://doi.org/10.1080/0305215X.2024.2447078.
7. Peiravi A, Nourelfath M, Zanjani M K. Redundancy strategies assessment and optimization of *k*-out-of-*n* systems based on Markov chains and genetic algorithms. Reliability Engineering & System Safety 2022; 221: 108277. https://doi.org/10.1016/j.ress.2021.108277.
8. Devi S, Garg H, Garg D. A review of redundancy allocation problem for two decades: bibliometrics and future directions. Artificial Intelligence Review 2023; 56(8): 7457–7548. https://doi.org/10.1007/s10462-022-10363-6.
9. Guilani P P, Ardakan M A, Dobani E R. Optimal component sequence in heterogeneous 1-out-of-N mixed RRAPs. Reliability Engineering & System Safety 2022; 217: 108095. https://doi.org/10.1016/j.ress.2021.108095.
10. Kim H. Markov-based reliability model for a mixed redundant system and parallel genetic algorithm with knowledge archives for a redundancy allocation problem. Reliability Engineering & System Safety 2023; 240: 109585. https://doi.org/ 10.1016/j.ress.2023.109585.
11. Jiang Y, Liu Z, Chen J H, Yeh W C, Huang C L. A novel binary-addition simplified swarm optimization for generalized reliability redundancy allocation problem. Journal of Computational Design and Engineering 2023; 10(2): 758–72. https://doi.org/10.1093/jcde/qwad021.
12. Zhang J, Lv H, Hou J. A novel general model for RAP and RRAP optimization of k-out-of-n: G systems with mixed redundancy strategy. Reliability Engineering & System Safety 2023; 229: 108843. https://doi.org/10.1016/j.ress.2022.108843.
13. Li X Y, Li X, Feng J, Li C, Xiong X, Huang H Z. Reliability analysis and optimization of multi-phased spaceflight with backup missions and mixed redundancy strategy. Reliability Engineering & System Safety 2023; 237: 109373. https://doi.org/10.1016/j.ress.2023.109373.
14. Yeh W C, Zhu W, Tan S Y, Wang G G, Yeh Y H. Novel general active reliability redundancy allocation problems and algorithm. Reliability Engineering & System Safety 2022; 218: 108167. https://doi.org/10.1016/j.ress.2021.108167.
15. Yeh W C. BAT-based algorithm for finding all Pareto solutions of the series-parallel redundancy allocation problem with mixed components. Reliability Engineering & System Safety 2022; 228: 108795. https://doi.org/10.1016/j.ress.2022.108795.
16. Oszczypała M, Ziółkowski J, Małachowski J. Redundancy allocation problem in repairable *k*-out-of-*n* systems with cold, warm, and hot standby: A genetic algorithm for availability optimization. Applied Soft Computing 2024; 165: 112041. https://doi.org/10.1016/j.asoc.2024.112041.
17. Oszczypała M, Konwerski J, Ziółkowski J, Małachowski J. Reliability analysis and redundancy optimization of *k*-out-of-*n* systems with

random variable *k* using continuous time Markov chain and Monte Carlo simulation. Reliability Engineering & System Safety 2024; 242: 109780. https://doi.org/10.1016/j.ress.2023.109780.

18. Li S, Chi X, Yu B. An improved particle swarm optimization algorithm for the reliability–redundancy allocation problem with global reliability. Reliability Engineering & System Safety 2022; 225: 108604. https://doi.org/10.1016/j.ress.2022.108604.
19. Zhang J, Lyu H, Hou J. Reliability optimization model for k-out-of-n:G systems based on mixed redundancy strategy. Computer Integrated Manufacturing System 2023; 29(3): 852. https://doi.org/10.13196/j.cims.2023.03.015.
20. Reihaneh M, Abouei Ardakan M, Eskandarpour M. An exact algorithm for the redundancy allocation problem with heterogeneous components under the mixed redundancy strategy. European Journal of Operational Research 2022; 297(3): 1112–25. https://doi.org/10.1016/j.ejor.2021.06.033.
21. Gholinezhad H. A new model for reliability redundancy allocation problem with component mixing. Reliability Engineering & System Safety 2024; 242: 109815. https://doi.org/10.1016/j.ress.2023.109815.
22. Peiravi A, Ardakan M A, Zio E. A new Markov-based model for reliability optimization problems with mixed redundancy strategy. Reliability Engineering & System Safety 2020; 201: 106987. https://doi.org/10.1016/j.ress.2020.106987.
23. Ge H, Gao H, Li X. Reliability optimization of reliability-redundancy allocation problems based on K-mixed strategy. Proceedings of the Institution of Mechanical Engineers, Part O: Journal of Risk and Reliability 2025; 239(4): 786–801. https://doi.org/10.1177/1748006X241272814.
24. Long Z, Ma Y, Cao E, Liang X. System reliability optimization under dynamic mixed heterogeneous redundancy strategy. Reliability Engineering & System Safety 2026; 268: 111969. https://doi.org/10.1016/j.ress.2025.111969.
25. Li X, Qin S, Liu K, Li Y. Reliability modeling and optimization of K/N phased mission system with backup missions and global redundancy strategy. Quality and Reliability Engineering International 2024; 40(2): 1061–78. https://doi.org/10.1002/qre.3456.
26. Li J, Wang D, Yang H, Liu M, Si S. An exact algorithm for RAP with *k*-out-of-*n* subsystems and heterogeneous components under mixed and K-mixed redundancy strategies. Advanced Engineering Informatics 2025; 65: 103163. https://doi.org/10.1016/j.aei.2025.103163.
27. Najmi A, Guilani P P. Optimization of a bi-objective reliability redundancy allocation problem with heterogeneous components and strategy selection. Computers & Industrial Engineering 2025; 209: 111438. https://doi.org/10.1016/j.cie.2025.111438.
28. Feng J, Chen ZL, Che A, Chu C. Exact MILP Models for Redundancy Allocation with Mixed Components. INFORMS Journal on Computing 2025. https://doi.org/10.1287/ijoc.2024.0842.
29. Sharifi M, Sayyad A, Taghipour S, Abhari A. Optimizing a joint reliability-redundancy allocation problem with common cause multi-state failures using immune algorithm. Proceedings of the Institution of Mechanical Engineers, Part O: Journal of Risk and Reliability 2023; 237(1): 152–165. https://doi.org/10.1177/1748006x221078128.
30. Oszczypała M. Bi-objective redundancy allocation problem in systems with mixed strategy: NSGA-II with a novel initialization. Reliability Engineering & System Safety 2025; 263: 111279. https://doi.org/10.1016/j.ress.2025.111279.
31. Bakhtiari M M, Amiri A, Sogandi F. A Fuzzy Multi-Objective Optimization for Series-Parallel Redundancy Allocation Problem Considering Mixed Redundancy Strategy. International Journal of Reliability, Quality and Safety Engineering 2025; 32: 2550014. https://doi.org/10.1142/S0218539325500147.
32. Lotovskyi E, Teixeira A P, Guedes C S. Availability analysis of an offshore oil and gas production system subjected to age-based preventive maintenance by Petri Nets. Eksploatacja i Niezawodność–Maintenance and Reliability 2020; 22(4): 627–637. https://doi.org/10.17531/ein.2020.4.6.
33. Duan R, Zhong Q, Lin Y, Zou Z, Cheng G, Zhou T. Reliability Assessment of Hybrid Hardware-Software Fault Systems Based on GSPN Under Mixed Uncertainties. Quality and Reliability Engineering International 2025; 41(8): 3622–3638. https://doi.org/10.1002/qre.70053.
34. Song Y, Mi J, Cheng Y, Bai L, Chen K. A dependency bounds analysis method for reliability assessment of complex system with hybrid uncertainty. Reliability Engineering & System Safety 2020; 204: 107119. https://doi.org/10.1016/j.ress.2020.107119.
35. Farh H M H, Al-Shamma'a A A, Alaql F, Omotoso H O. Optimization and uncertainty analysis of hybrid energy systems using Monte Carlo simulation integrated with genetic algorithm. Computers and Electrical Engineering 2024; 120: 109833. https://doi.org/10.1016/j.compeleceng.2024.109833.
36. Chib S, Greenberg E. Understanding the metropolis-hastings algorithm. The American Statistician 1995; 49(4): 327–335.

https://doi.org/10.1080/00031305.1995.10476177.

37. Hill S D, Spall J C. Stationarity and convergence of the metropolis-hastings algorithm: Insights into theoretical aspects. IEEE Control Systems Magazine 2019; 39(1): 56–67. https://doi.org/10.1109/MCS.2018.2876959.
38. Wang H. A Multi-Objective Strategy for Solving the Redundancy Allocation Problem in Reliable Systems via the NSGA-II Algorithm. Eksploatacja i Niezawodność – Maintenance and Reliability 2026; 28(3): 218332. https://doi.org/10.17531/ein/218332.

Acronym

RAP	Redundancy Allocation Problem
GSPN	Generalized Stochastic Petri Nets
MCS	Monte Carlo Simulation
GA	Genetic Algorithm
FS-GA	fixed-random-seed Genetic Algorithm
CTMC	Continuous-Time Markov Chain
MCMC	Markov Chain Monte Carlo
MTTF	Mean Time To Failure
CDF	Cumulative Distribution Function
TFN	Triangular Fuzzy Number
N	No Redundancy
A	Active Redundancy
S	Cold Standby Redundancy
M	Mixed Redundancy
R-RAP	Reliability-Redundancy Allocation Problem